# CHAPTER 4

# Application to Fission Gas Release

## 4.1 Problem Overview

In the previous chapters collocation-based and Kriging surrogates were applied to several play problems in hopes of demonstrating the surrogates' efficacy. Ultimately, the same surrogate methods will be applied to a difficult problem in nuclear fuel performance modeling. Specifically, modeling the depletion behavior of high burnup fuel is of interest. The field of fuel performance modeling is an ideal application for surrogates because most modern fuel performance codes such as Bison [66] are computationally expensive and there is a relative abundance of experimental data to complement the computer codes. Recall that the true promise of surrogates arises when thousands of simulations of an expensive computer code are required, as is the case for optimization and calibration studies. The idea is to fold together computer simulations and experimental data to improve the computer code's predictive accuracy.

Calibration studies involving the fuel performance code Bison have already been conducted by Swiler et. al. in [58]. In [58], an optimal fuel relocation activation parameter is identified by an aggregated calibration to experimental observations of several Halden fuel rods. Surrogates were not required for the calibration study due to the relative simplicity of the fuel rod model used. The Dakota [2] framework was used to complete the calibration study.

For the proposed thesis research the application of interest arises from the extensive validation base for fuel performance modeling found in the Fumex-II database [38]. Specifically, the application involves calibrating fission gas parameters involved in modeling the Risø AN3 experiment since these parameters are notoriously uncertain. The Risø AN3 experiment consists of a base irradiation of four reactor cycles, as shown in Fig. 4.1 followed by a power ramp. The base irradiation takes place in the Biblis A pressurized water reactor [38]. After the base irradiation period, a fuel rod is extracted and refabricated to

Figure 4.1: Base irradiation history for the Risø AN3 experiment.

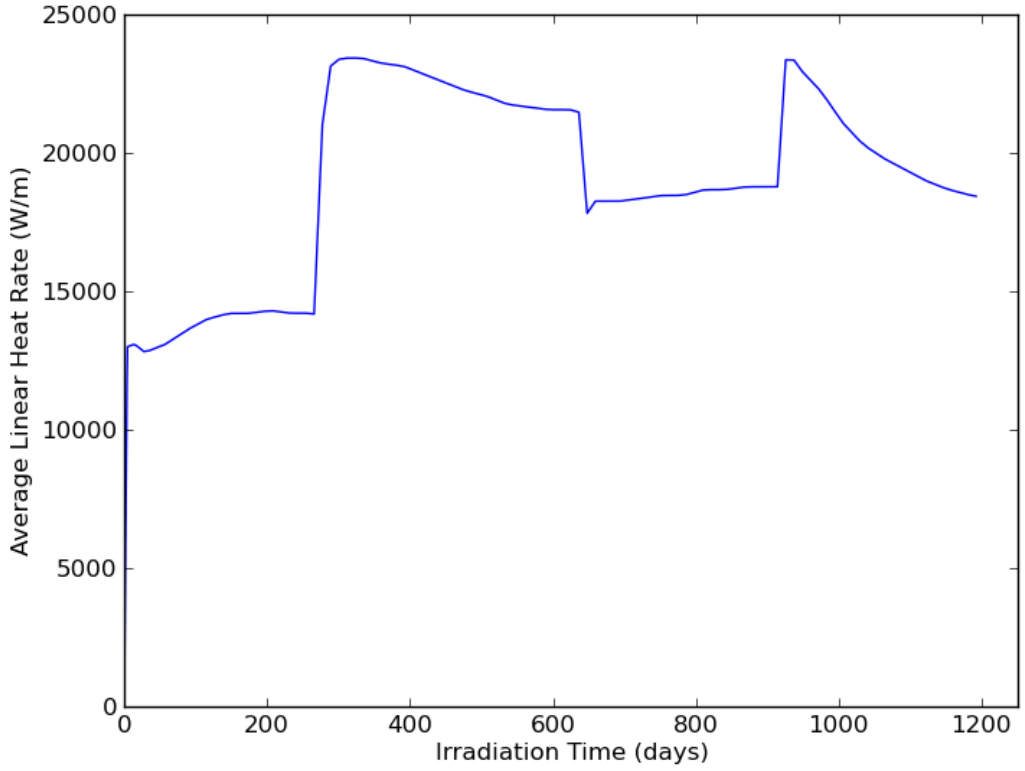

Figure 4.2: Power ramp experiment for the the Risø AN3 experiment.

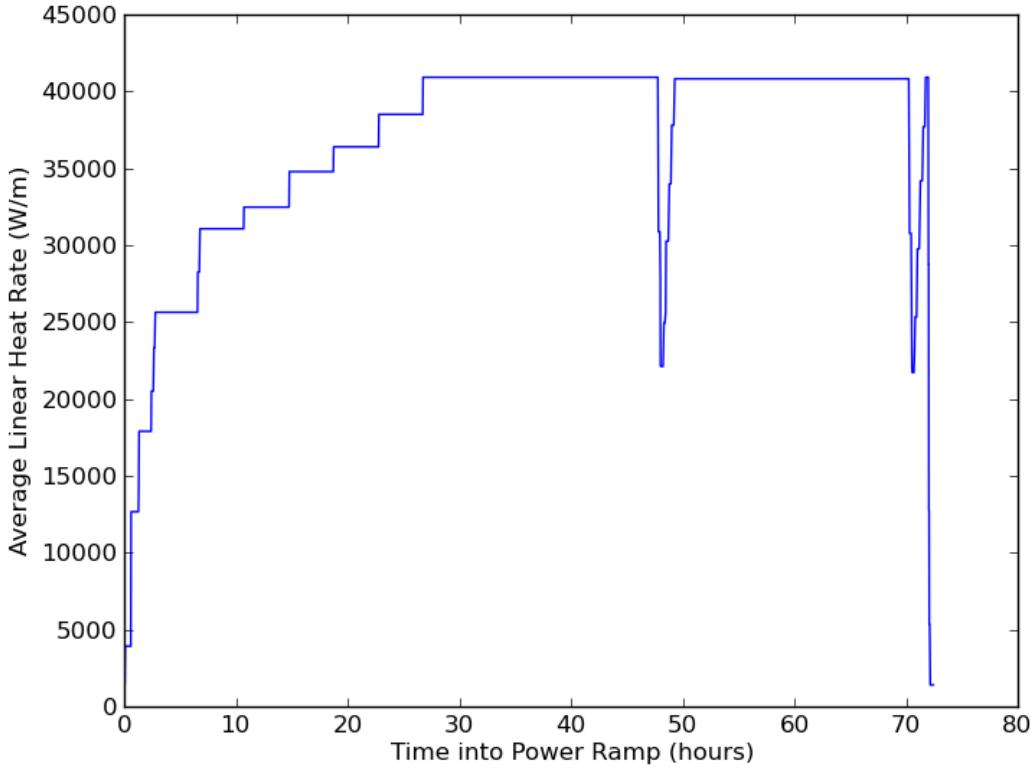


a shorter length before undergoing the power ramp in Fig. 4.2. The refabricated fuel rod is outfitted with various instrumentation such that fuel centerline temperature, fission gas release and rod internal pressure measurements can be obtained.

The Risø AN3 experiment was modeled using solely Bison in [51]. To model fission gas release the SIFGRS model is utilized. Bison's prediction of fission gas release during the power ramp is displayed alongside the corresponding experimental results in Fig. 4.3. As seen in Fig. 4.3, Bison over predicts fission gas release by a factor of two some forty hours into the power ramp. Similarly, Bison's prediction of fuel centerline temperature is plotted against experimental data in Fig. 4.4. Since fission gas release and fuel temperature are strongly coupled [51], it is anticipated that better fission gas release predictions will result in a more accurate fuel centerline temperature comparison.

Calibrated parameters in SIFGRS are expected to decrease the error between Bison's predicted output and the experimental data. Input parameters to SIFGRS such as the fuel grain radius, hydrostatic stress, fuel porosity, bubble surface tension, and the gas diffusion

Figure 4.3: Comparison of Bison fission gas release prediction to experimental results during the Risø AN3 power ramp.

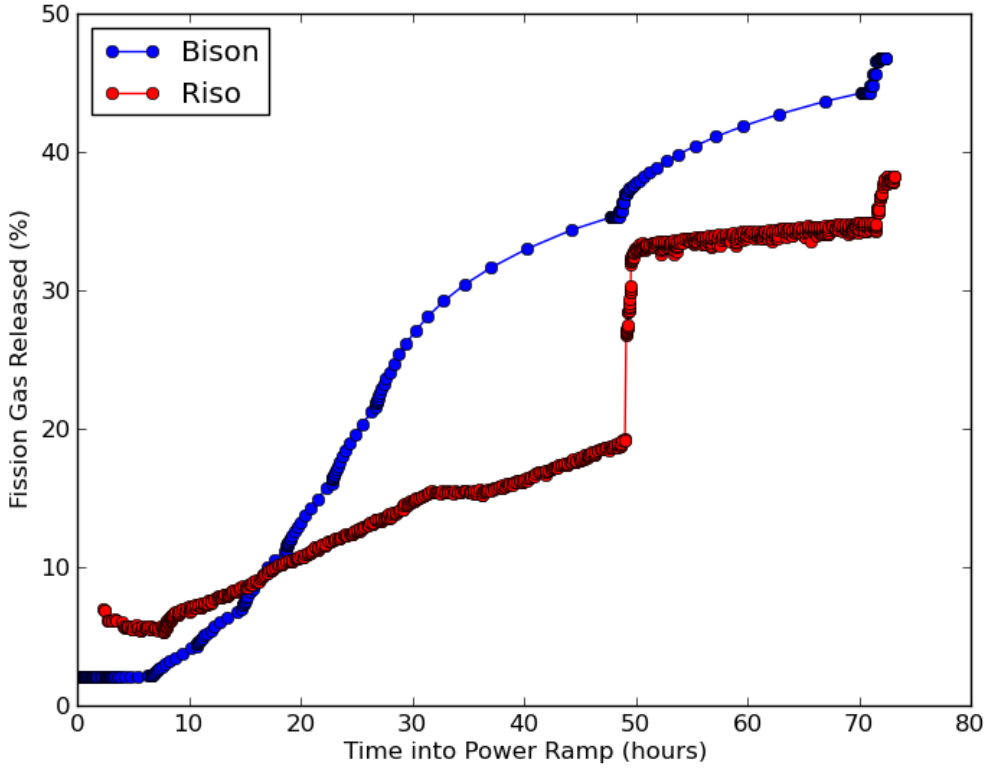

Figure 4.4: Comparison of Bison fuel centerline temperature prediction to experimental results during the Risø AN3 power ramp.

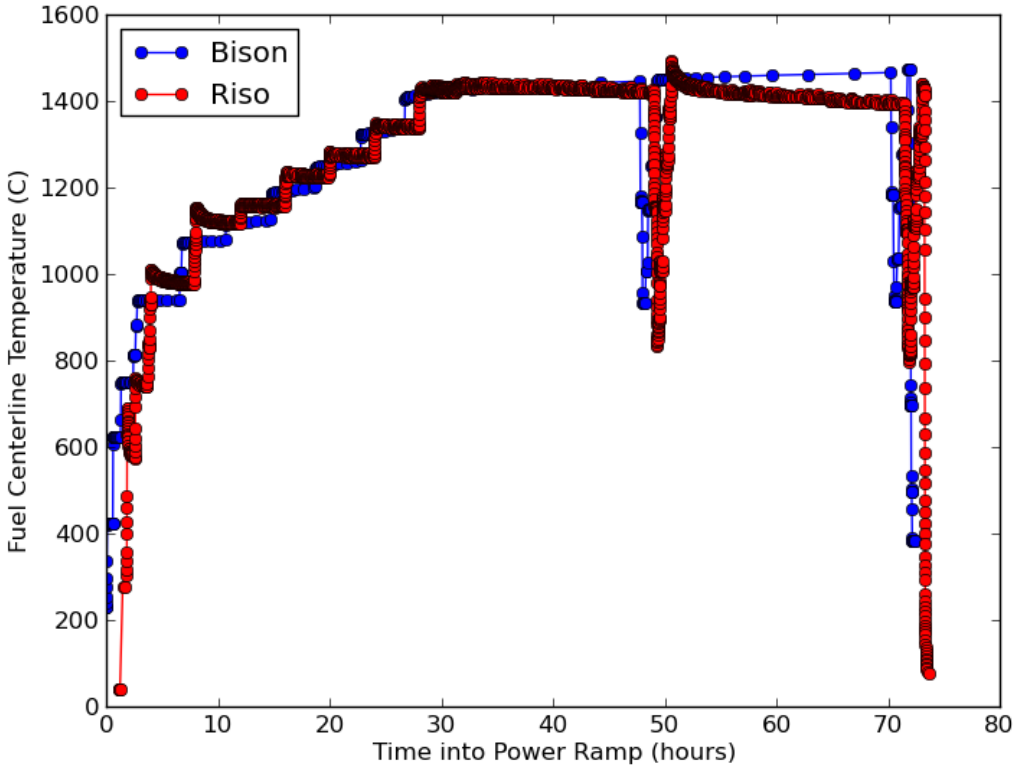


coefficient are quite generic and uncertain. Consequently, adjusting such parameters to better match experimental data is justified. However, Bison's fission gas release predictions are computationally expensive. Considering the calibration of parameters in SIFGRS will requires thousands of Bison instances, a surrogate model for fission gas release behavior becomes necessary. As in [56], the Dakota framework will be utilized to construct surrogate models for fission gas release behavior and to perform calibration routines.

The primary culprits in the SIFGRS model have been identified in [57] and [50] to be the initial fuel grain radius, fuel porosity, surface tension, temperature, fuel grain radius, diffusion coefficient, resolution parameter and grain boundary coefficient. The importance and role of of these variables will be described in section 4.2. For now, suffice it to say that the true values of these variables are unknown and only uniform probability distributions can be attached to each variable. As a starting point for analysis, the LHS module in Dakota was utilized to sample the variable space and simulate the resulting fission gas release time

Figure 4.5: Fission gas release time series for 100 LHS Bison simulated Risø AN3 power ramp experiments.

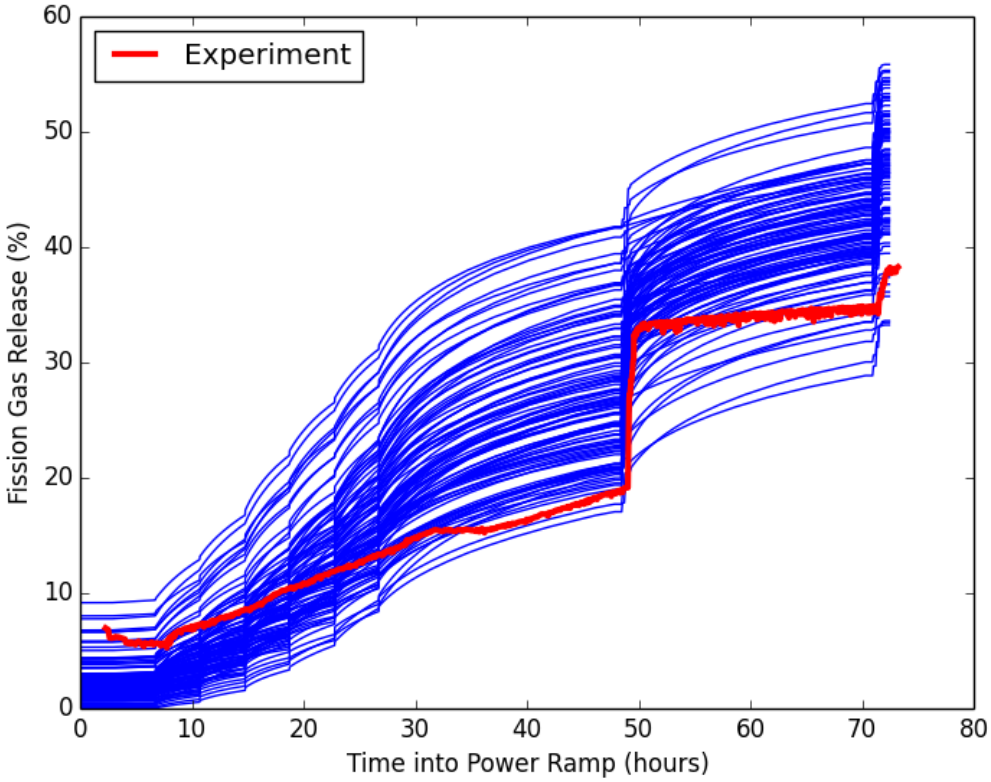


series resulting from the Risø AN3 power ramp. The 100 resulting time series are shown in Fig. 4.5. From Fig. 4.5, it is clear that Bison tends to over predict fission gas release. However, it is also apparent that the range of variables is sufficient to contend with the experimental data.

## 4.2 Fission Gas Release Theory

## 4.3 Kriging Surrogate

### 4.3.1 Insights with Principal Component Analysis

The problem at hand involves a time-dependent objective function, namely the fission gas release fraction throughout the course of a power ramp. Considering most surrogate

methodologies, including the ones of interest in this thesis, are designed to handle single objective functions at a time, constructing a surrogate for an entire time series is problematic since a surrogate must be constructed at every time step. Such is especially the case when one does not know a priori whether or not a given time series will contain interesting features mid-cycle, such as jumps and peaks in the objective function. In addition, if pertinent experimental time series data is available and a calibration study is desired, a surrogate model for the entire time series will be necessary. Time dependency is not an issue if one is only interested in investigating, for example, beginning of life or end of life behavior.

As with many of the great ideas in linear algebra, the premise of PCA rests on a change of basis. PCA attempts to represent some original data samples in terms of a set of basis vectors that reduce redundancy and noise in the data. To this end, consider a matrix $\mathbf{X}$ of $n$ observations and $k$ variables where the $k$ variables have been rescaled by their respective mean, as shown in Eq. 4.1. Rescaling by the mean will ensure that the projected data will live around the centroid of the new basis vectors.

$$\mathbf{X} = \begin{pmatrix} | & | & \cdots & | \\ X_1 & X_2 & \cdots & X_k \\ | & | & \cdots & | \end{pmatrix} \tag{4.1}$$

The problem PCA solves is that of choosing a set of expansion coefficients $\{p_{1j}\}_{j=1}^{k}$ such that,

$$\mathbf{Y}_1 = \mathbf{p}_1^T \mathbf{X}^T = p_{11}X_1 + p_{12}X_2 + \cdots + p_{1k}X_k \tag{4.2}$$

captures the largest variance in the data set. In other words, $\mathbf{Y}_1$ will point in the direction of largest variance. To bound the potential values of $\mathbf{p}_1$ the condition $\|\mathbf{p}_1\|_2 = 1$ is enforced. Since it is unlikely that $\mathbf{Y}_1$ will capture all the variance in the data, PCA goes on to find $\mathbf{Y}_2, ..., \mathbf{Y}_k$ such that all the variance in the data is accounted for. Each $\mathbf{Y}_j$ is independent from the other $\mathbf{Y}_{i\neq j}$ to make sure there is no redundancy in capturing variance. Each $\mathbf{Y}_j$ is referred to as the $j$-principal component. In matrix form, the workings of PCA result in,

$$\mathbf{Y} = \mathbf{P}^T \mathbf{X}^T. \tag{4.3}$$

From Eq. 4.3 it becomes clear that the operator $\mathbf{P}$ consisting of $\{p_{ij}\}_{i,j=1}^{k}$ has the effect of rotating the data in $\mathbf{X}$ onto an uncorrelated set of axis.

While the desired effect of operator $\mathbf{P}$ to produce output $\mathbf{Y}$ has been described, the question of how to find the expansion coefficients comprising $\mathbf{P}$ remains. As described in [54], the coefficients can be shown to be the loadings of the eigenvectors of the covariance

matrix for $\mathbf{X}$. The columns of $\mathbf{P}$ are the eigenvectors of the symmetric matrix,

$$\begin{pmatrix} \sigma_{1,1} & \sigma_{1,2} & \cdots & \sigma_{1,k} \\ & \sigma_{2,2} & \cdots & \sigma_{2,k} \\ & & \ddots & \vdots \\ & & & \sigma_{k,k} \end{pmatrix} \tag{4.4}$$

where $\sigma_{i,j}$ represents the covariance between random variables $X_i$ and $X_j$. The eigenvalues of the matrix in Eq. 4.4 represent the amount of variance covered by the respective eigenvector. Before being placed into $\mathbf{P}$, the eigenvectors should be sorted in descending order with respect to eigenvalue.

The utility of PCA lays in the fact that for most data sets the variance can be projected onto $\mathcal{O}(1)$ eigenvectors. To reveal this property the sorted eigenvalues can be plotted consecutively. PCA can be viewed as a tool for reducing the dimensionality of a data set by opting to keep only the first $r$-principal components since a majority of the variance can be projected onto these components. Indeed, if only $r$ eigenvectors are kept then the projected data can written as,

$$\mathbf{Y}_r = \mathbf{P}_r^T \mathbf{X}^T. \tag{4.5}$$

Using Eq. 4.5 the reduced-variance version of the data in $\mathbf{X}$ can be reconstructed as,

$$\mathbf{X}_*^T = \mathbf{P}_r \mathbf{Y}_r \tag{4.6}$$

where it's noted that the inverse of a matrix with orthonormal columns is its transpose. The reconstructed data in Eq. 4.6 represents perturbations around a centroid; the data mean must be added back in to obtain physical values. Using PCA to express a data set in terms of a more meaningful and truncated basis allows one to filter out noise and identify structure in the data. Such possibilities allow one to glean insights into the main contributors of a data set's variance [8].

To obtain insight into the contributors of variance in Bison fission gas release time series, PCA is applied to the data shown in Fig. 4.5. Each of the 100 time series shown in Fig. 4.5 is induced by a different set of SIFGRS parameters. Consequently, the time-stepping required for convergence in Bison varies from one time series to another. To perform PCA on the data, fission gas release fractions must be compared at identical times throughout the 100 different samples. Consequently every power ramp time series output by Bison is interpolated using cubic splines and then sampled at 150 evenly spaced points. The covariance matrix central to PCA in this case contains covariances between all 150

Figure 4.6: Cummulative variance carried by successive eigenvalues in the PCA covariance matrix.

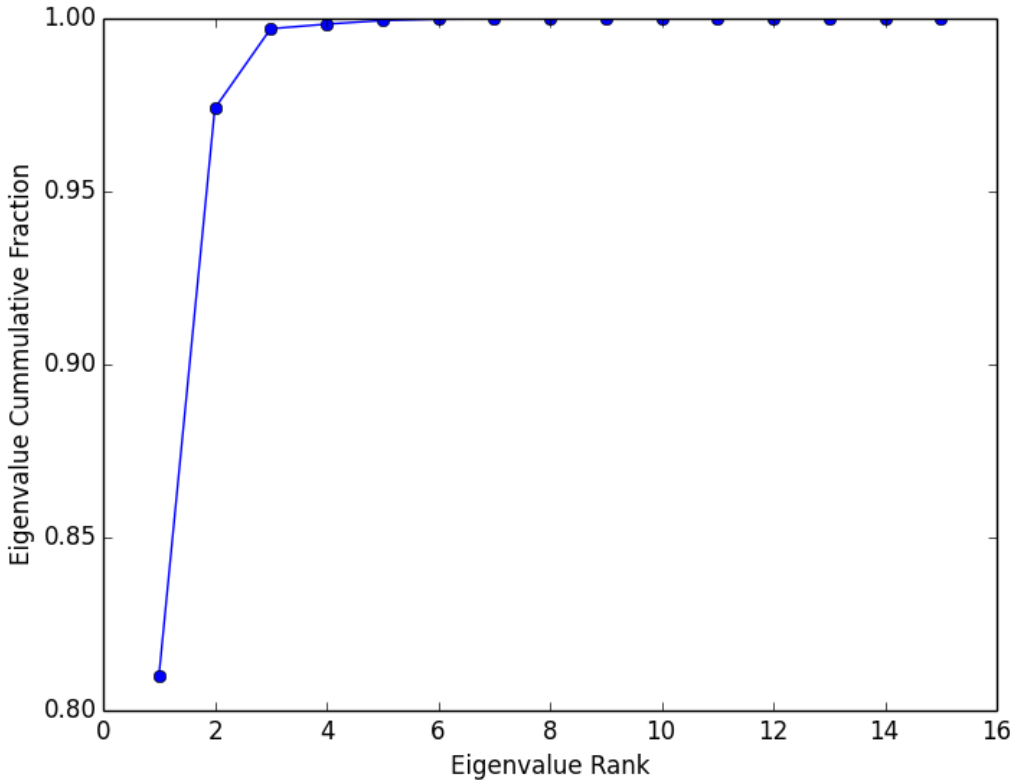


time steps. The eigenvalues of the covariance matrix are depicted in Fig. 4.6. As seen in Fig. 4.6, the three largest eigenvalues account for over 99% of the variance. If the original time series data is rotated onto the corresponding three principal components using Eq. 4.5, each time series can be represented using only three expansion coefficients. Consequently, surrogates can be constructed for only the three expansion coefficients as a function of the SIFGRS parameters. Instead of having to construct a surrogate at every time step, the principal component expansion coefficient surrogates act as a mapping to the entire time series.

The three principal components corresponding to the three largest eigenvalues of the time series covariance matrix are plotted in Fig. 4.7. The principal components enable insight into an underlying stochastic process by observing the magnitude of their coefficients [8]. Each time index's magnitude in a principal component represents its influence on the component. From Fig. 4.7 it appears as though the first principal component is

Figure 4.7: First three principal components of the time series covariance matrix.

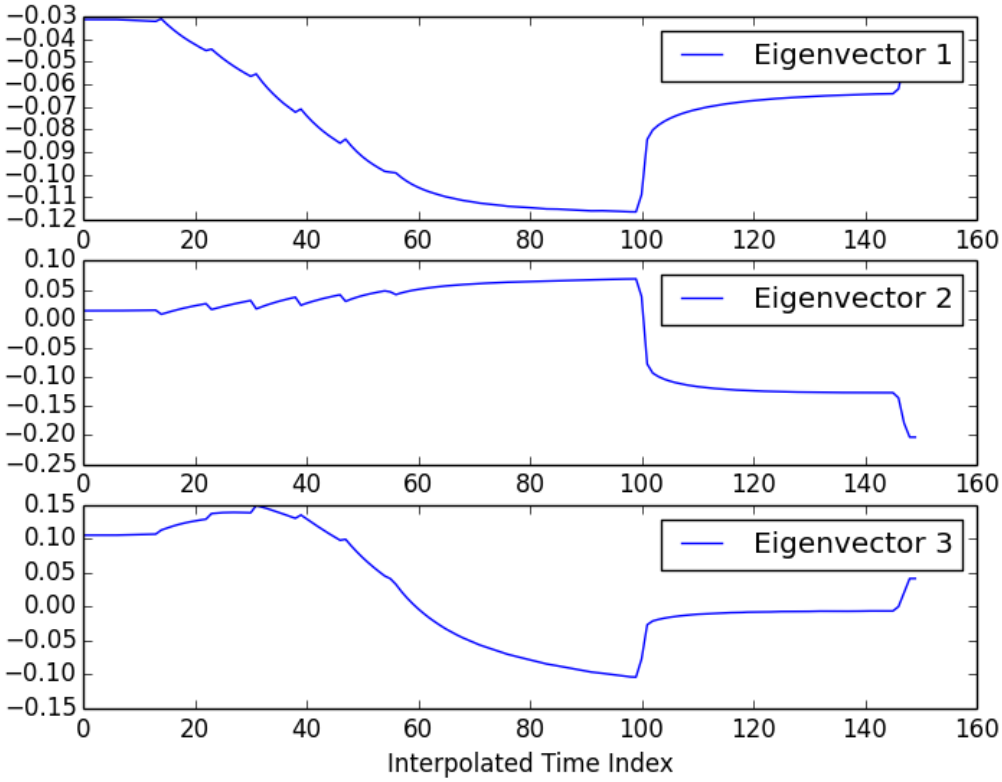

Figure 4.8: Time series of the first principal component and correlations with SIFGRS parameters.

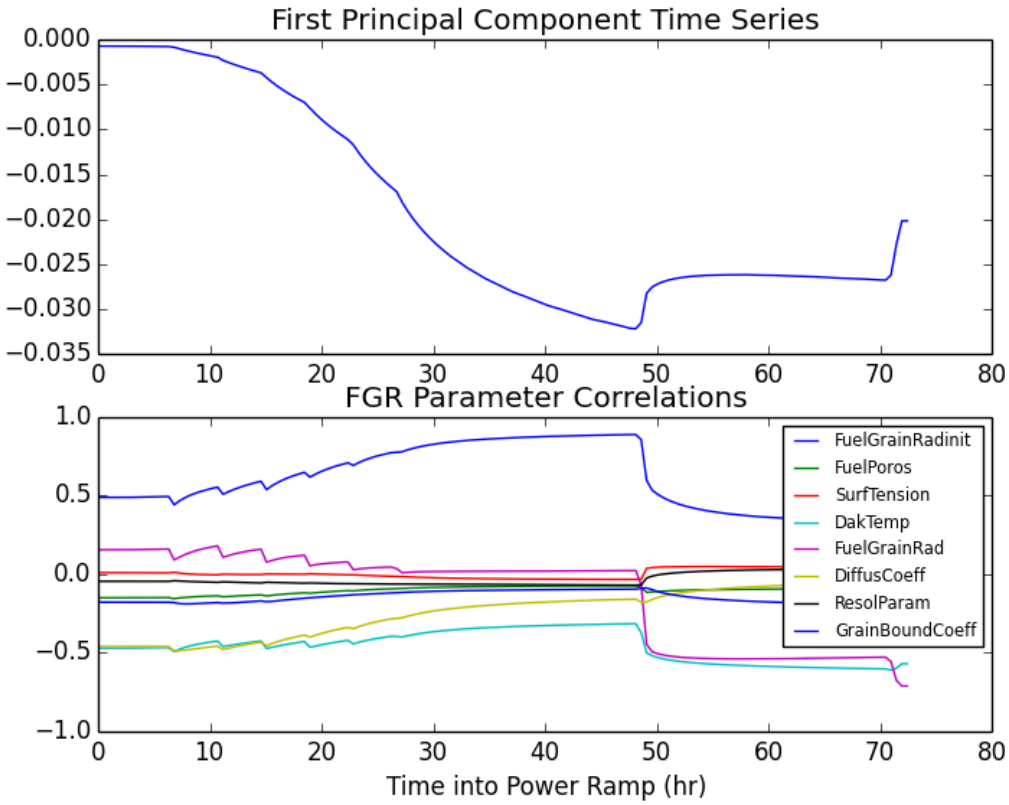


strongly influenced by the times in the middle of the power ramp, the second principal component is influenced by the times at the end of the power ramp and the third principal component is influenced most by the early stages of the power ramp. Further insights can be gleaned by plotting the principal components as time series and correlating the loadings with the LHS values for the SIFGRS parameters as in Fig. 4.8. The initial fuel grain radius appears to be the leading driver of the variance in the first principal component judging by its high correlation in the middle of the power ramp. Observe how in the late stages of the power ramp, the temperature and grain radius become primary contributors.

## 4.4 Collocation-based Surrogate

## 4.5 Analysis of Surrogate Performance